The IMOMM method opens the way for the accurate calculation of "real" transition metal complexes

Feliu Maseras

Unitat de Química Física, Edifici C.n, Universitat Autònoma de Barcelona, 08193 Bellaterra, Catalonia, Spain. E-mail: feliu@klingon.uab.es

Received (in Cambridge, UK) 1st August 2000, Accepted 16th August 2000
First published as an Advance Article on the web 4th September 2000

The Integrated Molecular Orbital Molecular Mechanics (IMOMM) method is spearheading the entry of hybrid quantum mechanics/molecular mechanics (QM/MM) approaches in computational transition metal chemistry. The high ratio between quality of results and computer cost offered by these methods allows the introduction, for the first time, of the full experimental complexes, in accurate calculations. Several chemically relevant topics in this way become available to theoretical consideration. This article reviews a few representative examples of these applications.

Introduction

Computational chemistry has made huge progress in recent decades.[1] It has gone from the qualitative explanation of chemical trends to the accurate calculation of physical properties. This evolution has been made possible in good part because of the ever-increasing power of computers and because of the development of new methods. Progress has been even more dramatic in the field of computational transition metal chemistry.[2,3] The relatively cheap Hartree–Fock methods, which are sufficiently precise for a good deal of organic chemistry, providing at least a reasonable starting point into the properties and reactivity of small organic molecules, are usually too inaccurate for transition metal chemistry. Transition metal compounds often require the introduction of correlation energy and relativistic effects for a qualitatively acceptable description. Methods including these features have not been readily available for systems of large size until the last decade.

There is nevertheless still a new dimension to be gained in computational transition metal chemistry, namely the full introduction of the complete ligands. Most of the calculations have traditionally made use of model ligands, with only the atoms directly attached to the metal being described as such. Typical examples of this practice would be the replacement of any phosphine by PH_3, or of any cyclopentadienyl derivative by C_5H_5. This approach has been successful because it provides a reasonable description of the metal–ligand bonding. However, there are a number of chemical features that depend on the specific nature of the ligand, and cannot be reproduced by these simplified models.

A very promising method for the introduction of the real ligands in theoretical calculations is the use of hybrid quantum mechanics/molecular mechanics (QM/MM) methods. In these methods, the system is divided in different regions, each of them with a different computational description, as shown for a particular example in Fig. 1. In this way, the interactions related to the bulk of the ligands, mostly of steric nature, can be appropriately treated with the much more affordable molecular mechanics approach. A complementary approach, the use of pure molecular mechanics, requires the development of a specific force field for each compound, or family of compounds, that are to be studied, and will not be discussed here.[5]

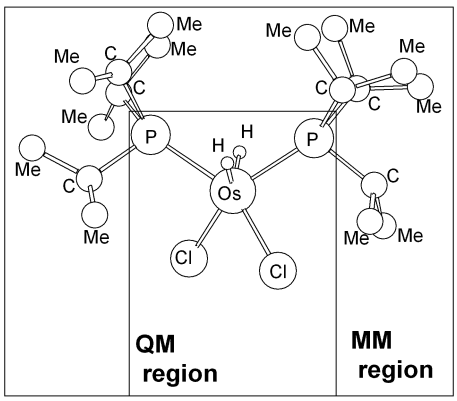

Fig. 1 Separation in QM and MM regions for an IMOMM calculation on $[OsCl_2H_2(PPr^i_3)_2]$.[4]

There are a variety of QM/MM methods proposed in the chemical literature, each with its particular methodological flavor.[6] This article will concentrate almost exclusively on the applications of one of them, Integrated Molecular Orbital Molecular Mechanics (IMOMM),[7] and of its derived forms.[8–10] This method has been so far the most widely applied to transition metal chemistry, mostly because of its robustness and simplicity. Precise descriptions of the method, and of its practical implementations can be found elsewhere.[7,11] Some aspects, like the mathematical treatment of the hydrogen bonds capping the dangling bonds in the QM region, which define the nature of different QM/MM methods, are still the subject of eventual improvement, but discussion of these aspects is outside the scope of this article,

There are nevertheless two characteristics of the IMOMM scheme that merit mention here because of their relevance in the

Feliu Maseras was born in 1962 in Martorelles, Catalonia. He studied at the Universitat Autònoma de Barcelona, where he obtained his B.Sc. in 1985 and his Ph.D. in 1991. He then spent two years as a postdoctoral fellow with Keiji Morokuma at the Institute for Molecular Science in Okazaki, Japan. After a two-year position as a CNRS Associate Researcher in the group of Odile Eisenstein in Montpellier, France, he took the position of Associate Professor at the Universitat Autònoma de Barcelona in 1998. His current research interests involve the development and application of theoretical methods to transition metal compounds, with special focus on the use of hybrid methods combining quantum mechanics and molecular mechanics for modeling species of experimental interest.

DOI: 10.1039/b006249i

interpretation and analysis of results. The first of these is that IMOMM is a full multistep method,[11] where the optimal geometry corresponds neither to the optimal QM arrangement nor to the optimal MM arrangement, but to the optimal, in a mathematical sense, compromise between both. The second defining characteristic of the IMOMM approach is that atoms in the MM region do not have a direct effect on the QM wavefunction, except through the distortions they induce in the geometry. Because of this, it can be stated that the IMOMM scheme introduces only the steric effects of the atoms in the MM region. On one hand, this supposes the introduction of an error, because the eventually important electronic contributions of these atoms are left out. On the other hand, this allows a straightforward separation between electronic and steric effects. The natural solution to the problem of electronic effects within the IMOMM scheme is the expansion of the QM region, which must include all electronic effects that are significant to the problem under study. As will be seen in the following sections, this can be used in some cases for the performance of computational experiments. Other QM/MM methods[6] introduce part of the electronic effects through the use of point charges. An alternative approach, available within the ONIOM scheme,[8] is the use of different quality QM descriptions for different regions of the systems.

A final methodological comment concerns the fact that the quality of IMOMM results, like that of any other QM/MM approach, depends critically on the appropriateness of the respective QM and MM methods to describe the interactions within the respective regions. Because of this, the quality of an IMOMM calculation is usually described in the form IMOMM(QM-method:MM-method), where the labels in parentheses describe the methods used in each of the two regions.

After this introduction, the current article focuses on a few selected applications of the IMOMM and related QM/MM methods to transition metal chemistry. The presentation does not intend to be exhaustive, but to be sufficiently general to show the possibilities of these methods to a general audience.

Structural studies

The most obvious feature of the application of hybrid QM/MM methods to transition metal chemistry is the possibility of introducing steric effects, and because of that a significant part of the published hybrid QM/MM calculations has been devoted to the analysis of how steric effects alter geometries and relative energies of transition metal complexes.

A representative study of how IMOMM calculations can be used in the identification of steric effects is provided by the joint experimental and theoretical study[12] on [Ir(biph)X(QR_3)$_2$] (biph = biphenyl-1,2-diyl; X = Cl, I; Q = P, As). These five-coordinate complexes have a distorted trigonal bipyramidal structure, as shown in Fig. 2. The phosphines (or arsines)

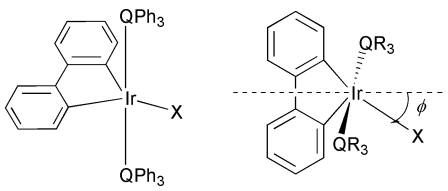

Fig. 2 Geometrical distortion of the equatorial X ligand in trigonal bipyramidal [Ir(biph)X(QR_3)$_2$] complexes.[12]

occupy the axial sites, and the halide and the chelating biph ligands are in the equatorial sites. A most intriguing feature of these compounds is the deviation that the halide presents from the symmetric arrangement between the two coordinating carbons of biph, a deviation characterized by values of φ (Fig. 2) different from zero. Previously reported calculations at the extended Hückel level suggested an electronic origin for the deviation. However, pure Becke3LYP calculations on the [Ir(biph)Cl(PH_3)$_2$] model system produced a symmetrical structure (φ = 0), making an electronic origin for the distortion unlikely.

The steric origin of the distortion was proved by IMOMM(Becke3LYP:MM3) calculations on the real system [Ir(biph)Cl(PPh_3)$_2$], which yielded a distortion angle φ of 11.4° (to be compared with the experimental value of 10.1°). The steric origin of the distortion shown by the hybrid QM/MM calculation was further confirmed by new experiments. In one of them, PPh_3 was replaced by $AsPh_3$, and in the other Cl was replaced by I. The logic behind these tests was that the modification of the size of the ligands should affect the importance of the steric effects, and therefore the value of the distortion angle. Values were merely indicative for [Ir(biph)Cl($AsPh_3$)$_2$] because of the presence of two different conformations of the arsine in the crystal structure, but clear for [Ir(biph)I(PPh_3)$_2$]. In this latter case the experimental value for the angle φ was 17.2°, 7.1° larger than for the parent compound, a trend reproduced by the corresponding IMOMM calculation. Therefore, the steric origin of the distortion from the electronically preferred symmetry was fully confirmed. Comparison of IMOMM and X-ray structures has allowed the characterization of steric effects also in [$ReH_5(PR_3)_2(SiR_3)_2$],[13] [$OsCl_2H_2(Pr^i_3)_2$],[4] and [Pd(P–N)($SiCl_3$)$_2$] (P–N = chiral chelating ligand).[14]

The application of hybrid QM/MM methods to structural problems is not restricted to the reproduction of crystal structures. A second block of structural studies has been centered in the evaluation of steric effects on the relative stabilities of two possible isomers. This type of work is well exemplified by the work on $Ru(CO)_2(PR_3)_3$,[15] where the study was centered in the comparison between the two isomers, *cis* and *trans*, as shown in Fig. 3. Both isomers have a trigonal

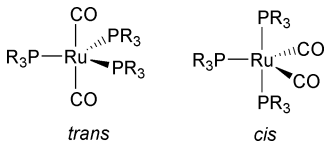

Fig. 3 The two isomers observed experimentally for $Ru(CO)_2(PR_3)_2$ complexes.[15]

bipyramidal geometry, and they are labeled following the arrangement of the two carbonyl ligands. The two forms have been observed experimentally[15,16] with different phosphine ligands PR_3. In particular, when PR_3 = PEt_3, the *cis* isomer is the species present in the crystal, with a C–Ru–C bond angle of 133.6°. When PR_3 = PPr^i_2Me, two independent molecules are present in the crystal, one of them of showing *trans* configuration (C–Ru–C 173.6°) and the other *cis* configuration (C–Ru–C 146.7°). IMOMM(MP2:MM3) calculations were carried out on these complexes using $Ru(CO)_2(PH_3)_3$ for the QM part. Both isomers, *cis* and *trans*, were found to be local minima for each complex. The computed C–Ru–C bond angles showed a clear separation between *trans* (178.2, 173.3°) and *cis* (136.7, 145.6°) forms, in good agreement with experimental data.

The most relevant part of this study was, however, comparison of the relative energies. For $Ru(CO)_2(PEt_3)_3$, the *cis* isomer, the only form existing in the crystal, was computed to be more stable than the *trans* isomer by 3.0 kcal mol^{-1}. The relationship between the two isomers is reversed for $Ru(CO)_2(Pr^i_2Me)_3$, the *trans* species being more stable by 2.8 kcal mol^{-1}. Electronic effects, represented by the QM energy, always favor the *cis* isomer, which has the two π-acceptor carbonyl ligands in equatorial positions. Steric effects, represented by the MM part, however, favor the *trans* isomer, with the three bulky phosphine ligands in equatorial positions. The

difference is that while electronic effects are similar for both PEt_3 and Pr^i_2Me, steric effects are significantly larger for the latter. As a result, the presence of the larger phosphine can invert the electronic preference for the *cis* isomer and make the *trans* isomer the most stable.

A similar IMOMM(Becke3LYP:MM3) study was carried out on $[MoO_2Cl_2(N–N)_2]$ (N–N = chelating ligand) complexes.[17] The nature of the adduct between $[OsHCl(CO)(PBu^t_2Me)_2]$ and $(CF_3)_2CHOH$ could also be clarified with the help of IMOMM(Becke3LYP:MM3) calculations.[18]

A final structural application of the IMOMM method to transition metal chemistry that will be analyzed in some more detail concerns the characterization of agostic interactions. An agostic interaction is the intramolecular interaction that takes place within one complex between the metal center and a C–H bond of one of the ligands.[19] Following their initial characterization, agostic interactions have been found to be very common in transition metal chemistry. They involve a three-center, two-electron bonding similar to that observed in main group Lewis acids such as diborane, and can also be viewed as an arrested state of the oxidative addition process of the C–H bond that would lead to the cyclometalated product. It follows that, from a molecular orbital point of view, the agostic interaction requires an empty orbital in the metal center, which must thus be unsaturated.

The steric repulsion associated with the presence of bulky ligands destabilizes high coordination numbers, also favoring unsaturated compounds. The coincidence of bulky ligands and agostic interactions in a number of complexes was therefore attributed mostly to its common association to unsaturated compounds. Recent hybrid QM/MM calculations have nevertheless proved a much more intimate relationship between steric influence and agostic interactions.[20–22]

A first proof of this relationship was obtained from the study, both experimental and theoretical, of the $Ir(H)_2(PBu^t)_2Ph)_2^+$ system (Fig. 4).[20] NMR and X-ray data showed the existence of

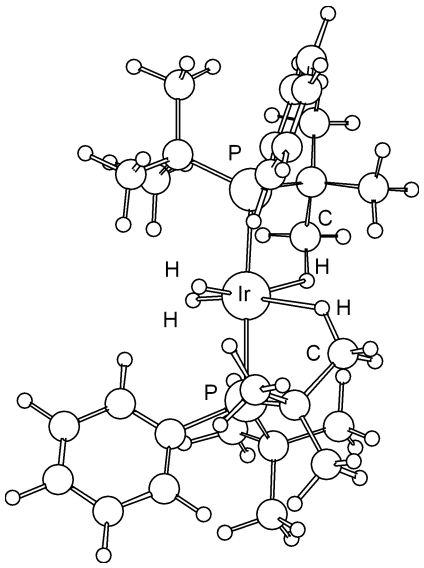

Fig. 4 IMOMM(Becke3LYP:MM3) optimized structure of $Ir(H)_2(PBu^t_2Ph)_2^+$.[20]

two agostic interactions in this complex, characterized geometrically by Ir–P–C angles of 97.0 and 99.0° (to be compared with Ir–P–C non-agostic angles of *ca.* 115°). Pure Becke3LYP calculations on $Ir(H)_2(PEtH_2)_2^+$ showed no agostic interactions at all (Ir–P–C angle of 118.4°). In contrast, IMOMM(Becke3LYP:MM3) calculations on the real complex using the same model for the QM part properly identified the agostic interactions (Ir–P–C angle of 101.7°). This result reveals two important consequences. The first is that the failure of the pure QM calculations on the model system means that the agostic interaction is intimately associated to the presence of the real ligands. The second consequence is that the success of the corresponding IMOMM calculation proves that the role of the ancillary substituents is steric in nature, and that the electronic contribution is at best minor.

While these first calculations on $Ir(H)_2(PBu^t_2Ph)_2^+$ clearly illustrated the importance of the introduction of the full ligand in the formation of the agostic interaction, they did not allow separation of the electronic and steric contributions to the steric distortion. This was accomplished within a systematic study of the steric influence on agostic interactions on a homologous series of Ir(III) complexes of general formula $Ir(H)_2(PR_3)_3^+$.[21] These complexes differ from that discussed above, with the presence of an extra phosphine, leading therefore to only one empty site in the coordination sphere, and one potential agostic interaction. In particular, the results for $Ir(H)_2(PCy_2Ph)_3^+$ are discussed. For this system, two different sets of partitioning of atoms between the QM and MM domains were applied in the IMOMM calculation (Fig. 5). In model I, all atoms not directly

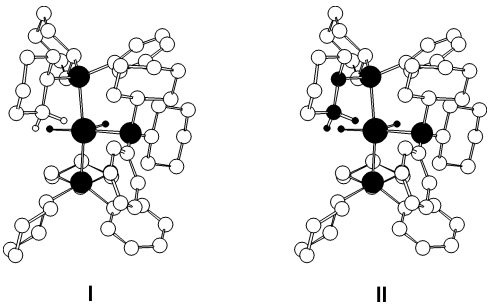

Fig. 5 The two different models used in IMOMM calculations on $Ir(H)_2(PR_3)_3^+$.[21] Atoms in the QM region are depicted in black.

bound to the metal were calculated at the MM level, the QM part being therefore $Ir(H)_2(PH_3)_3^+$. In model II, the QM part of the phosphine included the chain agostically distorted, the QM part thus being $Ir(H)_2(PEtH_2)_3^+$. The essential difference between each model is in the description of the potentially agostic C–H bond.

The geometry of $Ir(H)_2(PCy_2Ph)_3^+$ was fully optimized at four different computational levels, defined by the two different partitions and the use of MP2 and Becke3LYP methods for the QM part. Since IMOMM(MP2:MM3) led to slightly more accurate values, only these results will be discussed here. The IMOMM(MP2/I:MM3) calculation gave results essentially in agreement with the X-ray determined structure, with the largest discrepancy being in the value of 105.6° for the agostic Ir–P–C angle. This was larger than the experimental X-ray value of 100.9°, but already smaller than the computed average Ir–P–C value at this phosphorus center of 109.9°. This result is relevant because it proves that the bulk of the ligands alone is able to push one of the C–H bonds of the cyclohexyl group into the proximity of the metal atom even without any agostic orbital interaction. Use of the more elaborate model IMOMM(MP2/II:MM3), with the C–H bond in the QM part, led to results even closer to the X-ray values. The Ir–P–C bond angle improved to 99.8°, only 1.1° from the experimental value. This change proves that there is also an orbital contribution to the agostic interaction. The ability to determine the consequence of only one type of interaction is a strength of the hybrid method, which allows the execution of "computational experiments".

The accuracy of the hybrid QM/MM method in the characterization of this type of complex further proved by the calculation[21] on the isoelectronic $Ir(H)_2(PPr^i_2Ph)_3^+$ complex, with smaller phosphines, which is observed experimentally as non-agostic. This behavior is correctly reproduced by the IMOMM(MP2:MM3) calculation, which finds Ir–P–C bond angles of 115.7°. The successful application of the IMOMM method to the description of agostic interactions is not limited to late transition metals such as iridium, as proved by an

experimental and theoretical study[22] on $Tp^*Nb(Cl)(CHMe_2)$-(PhC≡CMe).

Homogeneous catalysis

The past two decades have witnessed the development of enantioselective catalysis both as a discipline and a production methodology in response to the increasing demand for enantiopure compounds for the pharmaceutical industry and the raising of environmental concerns.[23] Frequently, the key species in the catalytic cycle involves a metal atom chelated by a polyfunctional organic molecule. The role of the metal center is essential in offering neighbouring sites for coordination of the substrate and reagent molecules, and in providing a low energy pathway for their reaction. The selectivity of the reaction is however decided by the interactions involving enantiotopic groups in the polyfunctional organic ligand and the substrate, which give rise to energetically well differentiated diastereomeric transition states.

Homogeneous catalysis presents therefore two characteristics that make it especially appealing for hybrid QM/MM methods: the requirement of a high-level QM description for the metal center and its immediate environment, and the need to include in the calculation a large system that can only be introduced through an MM description. As a result, some of the more fruitful applications of the IMOMM method have been in the field of homogeneous catalysis.

Mechanisms for these processes are often complicated, and the interactions involved in enantioselectivity are often subtle. Because of this, and for the sake of the brevity of the article, the discussion will be concentrated on one of the reactions studied with the IMOMM method, the dihydroxylation of olefins by osmium tetroxide, with a brief mention made to other processes.

The osmium tetroxide-catalyzed dihydroxylation of olefins is a highly efficient method for the enantioselective introduction of chiral centers in organic substrates.[24] The reaction goes through an osmate ester intermediate containing a five-membered ring, and the stereoselectivity is decided in the formation of this intermediate after the initial interaction between catalyst and substrate. The mechanism for this part of the reaction has been the subject of intense discussion, and there seems to be finally an emerging consensus on the so-called [3 + 2] mechanism. A substantial role in the formation of this consensus has been provided by theoretical evidence from pure QM calculations on the $OsO_4(NH_3)$ + $H_2C{=}CH_2$ model system.[25]

Despite its relevance for the determination of the mechanism, calculations with the $OsO_4(NH_3)$ model cannot provide any explanation on the enantioselectivity of the reaction, because this property is related to the nature of the substituents in the NR_3 group, which are usually very bulky, as shown in the example presented in Fig. 6. A first preliminary IMOMM

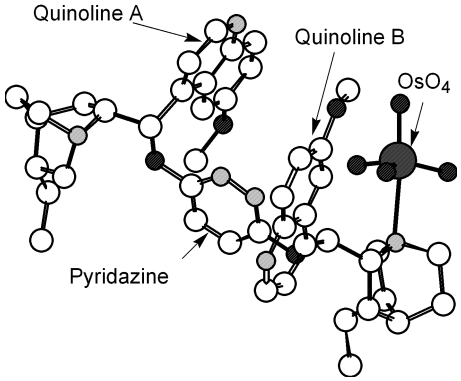

Fig. 6 Schematic presentation of the $(DHQD)_2PYDZ{\cdot}OsO_4$ catalyst.

study[26] on the subject consisted of the geometry optimization of the only two models of the catalyst where X-ray structures are available, namely $[OsO_4$(quinuclidine)] and [OsO_4\{(dimethylcarbamoyl)dihydroquinidine\}], and results showed an acceptable agreement with the experimental geometries.

The reaction of the catalyst with the olefin has been analyzed theoretically in detail in the case of the $(DHQD)_2PYDZ{\cdot}OsO_4$ [$(DHQD)_2PYDZ$ = 3,6-bis(dihydroquinidine)pyridazine] + $H_2C{=}CHPh$ system with the IMOMM(Becke3LYP:MM3) method using an $OsO_4(NH_3)$ + $H_2C{=}CH_2$ model for the QM part.[27,28] A first study[27] was concerned with the reaction profile of the formation of the osmate ester from the separated reactants. A likely reaction path leading to the experimentally observed *R* isomer was characterized though the location of the separate reactants, an intermediate, a transition state, and the product. Their relative energies, with respect to the reactants, were 0.0, −9.7, −3.3 and −34.3 kcal mol^{-1}, respectively. The geometries of both transition state and product were very similar to those obtained by pure QM calculations on the model system.[25] This proved the validity of the studies on the model system for the late stages of the reaction. The IMOMM study revealed nevertheless the presence of an intermediate that had not been located in the model system. The existence of this intermediate, shown in Fig. 7, is intimately associated to the

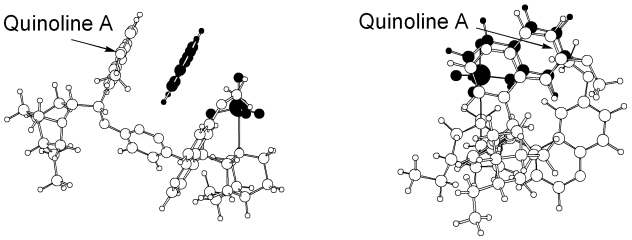

Fig. 7 IMOMM(Becke3LYP:MM3)-optimized[27] structure of the intermediate in the dihydroxylation of styrene catalyzed by $(DHQD)_2PYDZ{\cdot}OsO_4$.

interaction between the substrate and the bulky NR_3 ligand. The styrene substrate is sandwiched by two methoxyquinoline walls, with the parallel arrangement of the aromatic rings producing an attractive interaction. This interaction between substrate and catalyst has important implications on the reaction mechanism, because it is likely to be affected by the orientation of the catalyst. This point was clarified by the second study that is discussed below.

The second IMOMM(Becke3LYP:MM3) study[28] on the reaction of $(DHQD)_2PYDZ{\cdot}OsO_4$ with styrene was specifically focused on the origin of the enantioselectivity of the reaction. Because the selectivity is defined by the initial approach of the substrate to the catalyst, a number of possible pathways must be analyzed. There are twelve such paths, defined by the three possible regions (A, B and C) of approach of the substrate to the catalyst and the four possible orientations (I, II, III and IV) of the phenyl ring of the substrate within each region, as shown in Fig. 8. Each of these twelve possible pathways was theoretically

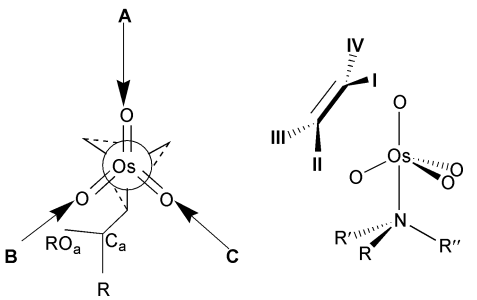

Fig. 8 Definition of the twelve possible reaction pathways in the reaction of $H_2C{=}CHPh$ with $(DHQD)_2PYDZ{\cdot}OsO_4$.

characterized through the location of the corresponding transition state, with its associated energy. The lowest energy saddle point, therefore the most likely transition state for the reaction, was B–I, followed closely by B–III and B–IV, 0.1 and 2.7 kcal mol^{-1} higher in energy. The next saddle point in energy,

A–IV, lies 4.7 kcal mol^{-1} above B–I. The fact that the three lowest energy saddle points correspond to region B, which is not the least sterically hindered (Fig. 8), is a clear indication that the non-bonding interactions between catalyst and substrate are of an attractive nature, in agreement with the existence of an intermediate.

The preference for paths B–I and B–III has an immediate consequence on the enantioselectivity of the reaction, because both lead to the *R* product. This is in excellent agreement with experimental data, that give a high enantiomeric excess of *R* product. In fact, all paths of type I and III go to the *R* product, while paths of type II and IV lead to the *S* product. The *S* product, which is a minor product of the reaction, must therefore come from path B–IV. Agreement with experiment reaches even to the value of the enantiomeric excess. If the ratio of products follows a Maxwell–Boltzmann distribution based on the internal energies of the transition states at 0 K, the theoretically computed enantiomeric excess would be 99%, close to the experimental value of 96%.

Application of hybrid QM/MM methods to the study of this reaction is not limited to the identification of the transition states and the reproduction of experimental data. It leads also to the analysis of the effect of the different regions of the catalyst on this enantioselectivity. The energy difference between the transition states, which is concentrated in the MM part of the calculation, can be further decomposed on a term by term basis. Grouping of the atoms in the regions of the catalyst according to the labels in Fig. 6 proves that the most decisive part in the selectivity (with a weight of *ca.* 50% of the interaction) is played by quinoline A, with significant, but smaller, contributions from quinoline B and pyridazine, and a very minor contribution from the OsO_4 unit.

The homogeneous catalysis process that has been the subject of more hybrid QM/MM calculations to date is however not dihydroxylation but olefin polymerization. This process had been traditionally carried out through heterogeneous catalysis, but several efficient homogeneous processes have gained importance in recent years.[29,30] Two major types of homogeneous catalysts are being used in this reaction, and both have been the subject of intense study through the IMOMM method. The most studied catalysts[31–33] have been those most recently developed, consisting of late transition metal complexes containing diimine ligands.[30] A typical QM/MM partition for these studies is shown in Fig. 9. The approach of the entering

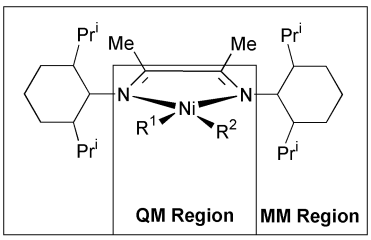

Fig. 9 Usual QM/MM partition applied in IMOMM calculations on the mechanism of olefin polymerization catalyzed by late transition metals.

monomer to the chain decides the general arrangement of the resulting polymer and, consequently, its physical properties. Calculations prove conclusively that this approach is controlled by the interactions of both fragments with the bulky substituents in the diimine group. It is worth mentioning that results of similar quality have been obtained in the application to related systems of different QM/MM combinations like IMOMM-(Becke3LYP:MM3),[31] IMOMM(BP:Amber)[32] and IMOMM(BP:CHARMM).[33] Apart from these studies on late-transition metal complexes, more traditional catalysts derived from bis-cyclopentadienyl complexes of early transition metals[29] have also been the subject of a number of IMOMM calculations.[34,35] All these calculations confirm that the tacticity and the chain length of the polymer are decided by steric interactions between substrate and catalyst. Both characteristics of the polymer depend on the relative values of the energy barriers for the insertion, branching and termination reactions. The values obtained for these processes from IMOMM calculations are in good agreement with experiment, and in an opposite order to that obtained in pure QM calculations on model systems.

A different catalytic process where hybrid QM/MM methods have made a recent entry is the enantioselective addition of diethylzinc to benzaldehyde promoted by chiral ligands.[36,37] Here, the RHF description is sufficient for the QM region, and the use of either UFF or MM3 descriptions in the MM region has provided satisfactory results. The IMOMM method has also been applied to the analysis of steric effects of bulky phosphine ligands on the mechanism of some particular reactions, such as the oxidative addition of hydrogen to $[Pt(PR_3)_2]$,[38] and the transformation of vinylidene to acetylene in the coordination sphere of $[RhCl(PPr^i_3)_2(C{=}CH_2)]$ complexes.[39]

Bioinorganic chemistry, heterogeneous catalysis, *etc*

The IMOMM method has found the most successful of its applications within transition metal chemistry in the two major fields described in the previous sections, where it is by far the most widely applied method. This notwithstanding, IMOMM and its modifications have also been applied to other areas of transition metal chemistry where other more elaborate QM/MM schemes have a well established tradition.

Biochemistry is probably the field where hybrid QM/MM schemes have found most of their applications. Proteins and nucleic acids have very large numbers of atoms, complicated folded structures, and both their structure and reactivities are heavily affected by the presence of water solvent molecules. The interaction with solvent molecules, which polarize the solute, is critical for a proper description of these systems, which consequently must introduce explicit polarization terms on the QM region.[6] Schemes like the original implementation of IMOMM,[7] where no polarization from the MM region is introduced in the QM region, are not adequate to the study of solvation problems, although the related ONIOM approach,[8] with a semiempirical description instead of MM should be appropriate.

The case of bioinorganic chemistry is however slightly different. There are a number of enzymes and proteins containing transition metals at their active center, with many atoms directly involved, and requiring the use of high level computational methods. The IMOMM method can be applied in this context to understand the properties of the active center, isolated from the rest of the protein. The analysis will be valid as far as the properties of the system are well reproduced in the isolated system, in a reasoning quite similar to that justifying experimental studies on biomimetic complexes. The performance of this approach can be seen in the example of IMOMM studies on complexes containing the heme group.

The heme group, constituted by an iron center and a porphyrin ring, occupies a prominent position in biochemistry as the active center of several relevant proteins and enzymes.[40] Although today computers allow calculation of the full heme group, the size of the system puts it at the limits of computer capacity, and hampers the performance of reactivity studies or very high level calibrations. An interesting alternative is the description of part of the porphyrin ring with an MM method.

The QM/MM partition used in the IMOMM calculations discussed here is presented in Fig. 10. In the QM part of the calculation the heme group is represented by $[Fe\{NH(CH)_3NH\}_2]$. The validity of the introduction of a QM/MM partition within the aromatic porphyrin ring is more arguable than in other topics previously discussed where the partition was across a single σ bond. One must however realize the fact that the four nitrogen donor atoms of the porphyrin are part of a large aromatic ring which has two different types of

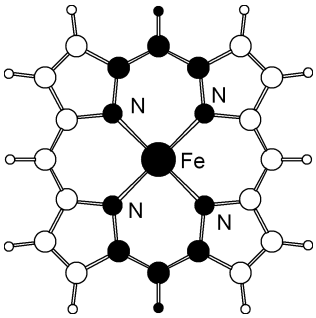

Fig. 10 QM/MM partition applied to the IMOMM calculation of iron porphyrin complexes. The QM atoms are depicted in black.

effects. One of those is the possibility that the aromatic ring has of acting as an electronic reservoir where occupied and empty orbitals are relatively close. This property is poorly reproduced in these IMOMM calculations. However, the other effect, the existence of a quite rigid framework, which precludes strong distortions out of planarity, is accurately described by the IMOMM calculation.

There was therefore a question on the reliability of this QM/MM modelization. This question was answered by a systematic set of calibrations,[41] where the results of the IMOMM calculation were compared with full *ab initio* and experimental data. Three different systems were analyzed, the four-coordinate [Fe(P)] (P = porphyrin) triplet system, the five-coordinate [Fe(P)(Im)] (Im = imidazole) quintet system, and the six-coordinate [Fe(P)(Im)(O_2)] singlet system. Computed IMOMM(Becke3LYP:MM3) geometries were always in reasonable agreement with those obtained from pure Becke3LYP calculations on the full systems, and with experimental X-ray crystal structure data on related species. The test was extended to the energy cost of the out of plane displacement of the iron atom. This factor, which ought to be ruled almost exclusively by electronic effects, *i.e.*, by the binding of the Fe center to the N atoms of the porphyrin ring, was examined with both pure Becke3LYP and IMOMM(Becke3LYP:MM3) calculations on the three different systems. The agreement of the values computed with both methods was good, with discrepancies smaller than 2 kcal mol^{-1} for displacements as large as 0.3 Å and as costly as 15 kcal mol^{-1}. Furthermore, the differences between the three different chemical systems were also well described, with the energy cost of a displacement of 0.3 Å being *ca.* 10 kcal mol^{-1} for the four-coordinate system, *ca.* 5 kcal mol^{-1} for the five-coordinate system and *ca.* 15 kcal mol^{-1} for the six-coordinate system. This QM/MM modeling of the heme group has been applied to the IMOMM(Becke3LYP:MM3) study[42] of the structural properties of [Fe(T_{piv}PP){1-Me(Im)}(O_2)], where T_{piv} is 5,10,15,20-tetrakis(α,α,α,α-*o*-pivalamidophenyl)porphyrin, a so-called picket-fence porphyrin.

A different example of application of IMOMM to bioinorganic problems is provided by the study of the catalytic mechanism of galactose oxidase.[43] In this case, the IMOMM method was used to introduce a backbone link between two residues attached to the copper center, a tyrosine and a histidine. The existence of the backbone is shown to affect the chemical nature of some reaction intermediates, but to have little effect on the overall energetics of the reaction.

Another field where QM/MM methods have been applied for a number of years is heterogeneous catalysis.[44,45] The simulation of a solid surface is much more affordable if one can describe at least part of it with an MM description. Some QM/MM methods have been specifically designed to deal with these chemical situations, and they have been applied with success to the case of zeolites.[44] Some success has also been obtained[46] in the application of IMOMM(Becke3LYP:MM3) calculations to the study of Cu atom deposition on SiO_2 surface defects. An IMOMM method that has been specifically designed for application to heterogeneous catalysis is the so-called SIMOMM (Surface IMOMM) method.[10] This method has been successfully applied to the description of the structure of the Si(001) surface[47] and to the cycloaddition reaction of cyclohexa-1,3-diene on this surface.[48] In this latter case, it has been shown that the presence of the bulk solid allows the possibility of a [2+2] reaction mechanism that was not available in gas phase studies on model reaction sites.

Concluding remarks

This article has shown how the IMOMM method, proposed only as recently as 1995, has already produced a significant amount of valuable theoretical contributions in transition metal chemistry. Its success has been logically concentrated in areas where the calculation of simplified models could not account for the experimental complexity, as in homogeneous catalysis and in structural issues associated with steric effects. Work in the area is nevertheless far from finished. There are many processes in transition metal chemistry where the bulk of the ligands seems crucial that have not as yet been tackled from a theoretical point of view. One must also expect developments from the methodological point of view. IMOMM is in fact a particular case of the more general ONIOM scheme,[8] which goes beyond the strict field of QM/MM methods by allowing the use of different QM descriptions, an approach that also has a role in transition metal chemistry.[49] Other developments in QM/MM methods will also find applications sooner or later to transition metal chemistry. In summary, the application of IMOMM and of other hybrid QM/MM methods to this field of chemistry looks very promising, and a sharp increase in the number of applications must be expected in forecoming years.

Acknowledgment

Profs. Keiji Morokuma (Emory), Odile Eisenstein (Montpellier) and Agustí Lledós (Barcelona) are thanked for helpful discussions throughout the years. Thanks must also be extended to the long list of graduate students and visitors in our group during recent years. Financial support from the Spanish DGES (Project No. PB98-0916-CO2-01) and DURSI (Generalitat de Catalunya) is acknowledged.

Notes and references

1 *The Encyclopedia of Computational Chemistry*, ed. P. v. R. Schleyer, N. L. Allinger, T. Clark, J. Gasteiger, P. A. Kollman, H. F. Schaefer and P. R. Schreiner, Wiley, New York, 1998.
2 E. R. Davidson, *Chem. Rev.*, 2000, **100**, 351.
3 *Computational Organometallic Chemistry*, ed. T. R. Cundari, Marcel Dekker, New York, 2000.
4 F. Maseras and O. Eisenstein, *New J. Chem.*, 1998, **22**, 5.
5 P.-O. Norrby, *J. Mol. Struct. (THEOCHEM)*, 2000, **506**, 9.
6 A. Warshel and M. Levitt, *J. Mol. Biol.*, 1976, **103**, 227; U. C. Singh and P. A. Kollman, *J. Comput. Chem.*, 1986, **7**, 718; M. H. Field, P. A. Bash and M. Karplus, *J. Comput. Chem.*, 1990, **11**, 700; J. Gao, *Acc. Chem. Res.*, 1996, **29**, 298; I. Tuñón, M. T. C. Martins-Costa, C. Millot, M. F. Ruiz-López and J.-L. Rivail, *J. Comput. Chem.*, 1996, **17**, 19; G. Monard and K. M. Merz, *Acc. Chem. Res.*, 1999, **32**, 904; Y. Zhang, H. Liu and W. Yang, *J. Chem. Phys.*, 2000, **112**, 3483.
7 F. Maseras and K. Morokuma, *J. Comput. Chem.*, 1995, **16**, 1170.
8 S. Humbel, S. Sieber and K. Morokuma, *J. Chem. Phys.*, 1996, **105**, 1959; S. Dapprich, I. Komáromi, K. S. Byun, K. Morokuma and M. J. Frisch, *J. Mol. Struct. (THEOCHEM)*, 1999, **461**, 1.
9 T. K. Woo, L. Cavallo and T. Ziegler, *Theor. Chem. Acc.*, 1997, **119**, 6177.
10 J. R. Shoemaker, L. W. Burggraf and M. S. Gordon, *J. Phys. Chem. A*, 1999, **103**, 3245.
11 F. Maseras, *Top. Organomet. Chem.*, 1999, **4**, 165.
12 G. Ujaque, F. Maseras, O. Eisenstein, L. Liable-Sands, A. L. Rheingold, W. Yao and R. H. Crabtree, *New J. Chem.*, 1998, **22**, 1493.
13 G. Barea, F. Maseras, Y. Jean and A. Lledós, *Inorg. Chem.*, 1996, **35**, 6401.
14 T. K. Woo, G. Pioda, U. Rothlisberger and A. Togni, *Organometallics*, 2000, **19**, 2144.

15 M. Ogasawara, F. Maseras, N. Gallego-Planas, K. Kawamura, K. Ito, K. Toyota, W. E. Streib, S. Komiya, O. Eisenstein and K. G. Caulton, *Organometallics*, 1997, **16**, 1979.
16 M. Ogasawara, F. Maseras, N. Gallego-Planas, W. E. Streib, O. Eisenstein and K. G. Caulton, *Inorg. Chem.*, 1996, **35**, 7468.
17 G. Barea, A. Lledós, F. Maseras and Y. Jean, *Inorg. Chem.*, 1998, **37**, 3321.
18 D. V. Yandulov, K. G. Caulton, N. V. Belkova, E. S. Shubina, L. M. Epstein, D. V. Khoroshun, D. G. Musaev and K. Morokuma, *J. Am. Chem. Soc.*, 1998, **120**, 12553.
19 M. Brookhart and M. L. H. Green, *J. Organomet. Chem.*, 1983, **250**, 395.
20 G. Ujaque, A. C. Cooper, F. Maseras, O. Eisenstein and K. G. Caulton, *J. Am. Chem. Soc.*, 1998, **120**, 361.
21 A. C. Cooper, E. Clot, J. C. Huffman, W. E. Streib, F. Maseras, O. Eisenstein and K. G. Caulton, *J. Am. Chem. Soc.*, 1999, **121**, 97.
22 J. Jaffart, R. Mathieu, M. Etienne, J. E. McGrady, O. Eisenstein and F. Maseras, *Chem. Commun.*, 1998, 2011.
23 *Comprehensive Asymmetric Catalysis*, ed. E. N. Jacobsen, A. Pfaltz and H. Yamamoto, Springer, Berlin, 1999.
24 H. C. Kolb, M. S. VanNieuwnhze and K. B. Sharpless, *Chem. Rev.*, 1994, **94**, 2483.
25 S. Dapprich, G. Ujaque, F. Maseras, A. Lledós, D. G. Musaev and K. Morokuma, *J. Am. Chem. Soc.*, 1996, **118**, 11660; U. Pidun, C. Boehme and G. Frenking, *Angew. Chem., Int. Ed. Engl.*, 1996, **35**, 2817.
26 G. Ujaque, F. Maseras and A. Lledós, *Theor. Chim. Acta*, 1996, **94**, 67.
27 G. Ujaque, F. Maseras and A. Lledós, *J. Org. Chem.*, 1997, **62**, 7892.
28 G. Ujaque, F. Maseras and A. Lledós, *J. Am. Chem. Soc.*, 1999, **121**, 1317.
29 H. H. Brintzinger, D. Fischer, R. Müllhaupt, B. Rieger and R. M. Waymouth, *Angew. Chem., Int. Ed. Engl.*, 1995, **34**, 1143.
30 L. K. Johnson, C. M. Killian and M. Brookhart, *J. Am. Chem. Soc.*, 1995, **117**, 6414.
31 R. D. J. Froese, D. G. Musaev and K. Morokuma, *J. Am. Chem. Soc.*, 1998, **120**, 1581; D. G. Musaev, R. D. J. Froese and K. Morokuma, *Organometallics*, 1998, **17**, 1850.
32 L. Deng, T. K. Woo, L. Cavallo, P. M. Margl and T. Ziegler, *J. Am. Chem. Soc.*, 1997, **119**, 6177; L. Deng, P. Margl and T. Ziegler, *J. Am. Chem. Soc.*, 1999, **121**, 6479; M. S. W. Chan, L. Deng and T. Ziegler, *Organometallics*, 2000, **19**, 2741; T. K. Woo, P. E. Blöchl and T. Ziegler, *J. Phys. Chem. A*, 2000, **104**, 121.
33 G. Milano, G. Guerra, C. Pellecchia and L. Cavallo, *Organometallics*, 2000, **19**, 1343.
34 G. Guerra, P. Longo, P. Corradini and L. Cavallo, *J. Am. Chem. Soc.*, 1999, **121**, 8651.
35 G. Moscardi, F. Piemontesi and L. Resconi, *Organometallics*, 1999, **18**, 5264.
36 B. Goldfuss, M. Steigelmann, S. I. Khan and K. N. Houk, *J. Org. Chem.*, 2000, **65**, 77.
37 J. Vàzquez, M. A. Pericàs, F. Maseras and A. Lledós, submitted to *J. Org. Chem.*
38 T. Matsubara, F. Maseras, N. Koga and K. Morokuma, *J. Phys. Chem.*, 1996, **100**, 2753.
39 Y. Wakatsuki, N. Koga, H. Werner and K. Morokuma, *J. Am. Chem. Soc.*, 1997, **119**, 360.
40 L. Stryer, *Biochemistry*, Freeman, New York, 1995.
41 J.-D. Maréchal, G. Barea, F. Maseras, A. Lledós, L. Mouawad and D. Perahia, *J. Comput. Chem.*, 2000, **21**, 282.
42 F. Maseras, *New J. Chem.*, 1998, **22**, 327.
43 F. Himo, L. A. Eriksson, F. Maseras and P. E. M. Siegbahn, *J. Am. Chem. Soc.*, 2000, **122**, 8031.
44 U. Eichler, C. M. Kölmel and J. Sauer, *J. Comput. Chem.*, 1996, **18**, 463.
45 A. H. de Vries, P. Sherwood, S. J. Collins, A. M. Rigby, M. Rigutto and G. J. Kramer, *J. Phys. Chem. B*, 1999, **103**, 6133.
46 N. Lopez, G. Pacchioni, F. Maseras and F. Illas, *Chem. Phys. Lett.*, 1998, **294**, 611.
47 J. R. Shoemaker, L. W. Burggraf and M. S. Gordon, *J. Chem. Phys.*, 2000, **112**, 2994.
48 C. H. Choi and M. S. Gordon, *J. Am. Chem. Soc.*, 1999, **121**, 11 311.
49 A. Sundermann, O. Uzan, D. Milstein and J. M. L. Martin, *J. Am. Chem. Soc.*, 2000, **122**, 7095.